LATVIAN JOURNAL OF PHYSICS
AND TECHNICAL SCIENCES
2026, N 3

DOI: 10.2478/lpts-2026-0017

ENHANCING ML PARTICLE DISTRIBUTION VIA SURFACE PEO IN COMPLEX METAL GEOMETRIES

E. Einbers[1]*, V. Vitola[1], A. Zolotarjovs[2]

[1]Institute of Solid State Physics,
University of Latvia,
8 Kengaraga Str., Riga, LV-1063, LATVIA
[2]Ltd. ElGoo Tech,
3-7 Vilandes Str., Riga, LV-1010, LATVIA
*e-mail: ernests.einbergs@cfi.lu.lv

Mechanoluminescence can be used as a contact-free visualisation of deformation, but particle integration in complex geometries is challenging. The paper demonstrates a proof-of-concept approach, in which plasma electrolytic oxidation (PEO) is used to create a porous alumina layer capable of hosting $SrAl_2O_4$: Eu, Dy mechanoluminescent particles on aluminium substrates. A 15-minute PEO treatment produced an optimal microstructure for particle retention and mechanical stability. While embedded particles showed limited mechanoluminescence due to outward pore expansion during bending, applying a thin epoxy glaze enabled strong and repeatable luminescent responses during both loading and unloading. The mechanoluminescence contrast ratio remained stable across long delay intervals, indicating robustness against afterglow decay. CMOS imaging confirmed the feasibility of spatial strain mapping, though surface inhomogeneity currently limits resolution. These results establish PEO-based particle integration as a promising route toward wire-free, full-field stress visualisation in metal components and highlight key microstructural factors for future optimisation.

Keywords: *Contact-free strain, mechanoluminescence, PEO, stress analysis.*

1. INTRODUCTION

Monitoring and analysing mechanical stress in metal components is critical for ensuring structural integrity and extending their lifespan. Excess internal stresses (for example, residual stresses introduced during manufacturing) can accelerate fatigue damage and precipitate unexpected failures if left unmonitored [1], [2]. To maximise the lifetime of metal parts, engineers must be able to detect and quantify mechanical stress that the metal part is subjected to, so that preventive maintenance can be implemented before catastrophic failure occurs. This need has driven the development of advanced stress measurement techniques in structural health monitoring and materials engineering. One emerging approach to stress sensing that does not require attached wires and sensors, involves mechanoluminescence – the phenomenon of light emission from a material under mechanical deformation [3].

Mechanoluminescent (ML) materials emit visible light in response to applied stress (a non-thermal process), and importantly for the application, the light intensity correlates strongly with the magnitude of stress. This behaviour enables ML materials to function as optical stress sensors: as the load on a structure increases, the material's luminescence becomes brighter, providing a visual map of stress distribution. For instance, Sohn et al. [4] observed that the well-known long afterglow luminophore $SrAl_2O_4$: Eu, Dy emits light under loading and can serve as a reproducible, non-destructive stress sensor. Such ML materials offer the possibility of full-field, contactless strain measurement. In our previous work we have started utilising this effect to visualise how stress is distributed in complex 3D printed parts in real time, which is particularly useful where conventional sensors are impractical [5], [6].

Plasma electrolytic oxidation (PEO) has emerged as a versatile technique for creating robust ceramic coatings on lightweight metals like aluminium. PEO (also known as micro-arc oxidation) uses high-voltage anodic sparks to grow a thick Alumina layer on the metal surface [7]. A key feature of PEO alumina is its porosity – the process inherently produces a porous oxide microstructure, with a characteristic bilayer architecture consisting of a dense inner oxide and a highly porous outer layer [7]. The porous network of the coating can be exploited to introduce functional materials into the surface – in one of our previous works we have incorporated $SrAl_2O_4$: Eu, Dy into PEO-formed oxide layers pores to create luminescent coatings [8]. This ability to host secondary particles or phases in the coating's pores opens the door to advanced multifunctional surfaces on metal parts.

In this study, we combine the concepts of mechanoluminescent sensing and PEO coating technology to develop a proof-of-concept optical method for real-time stress measurement in metal components. The approach involves first creating a porous alumina coating on an aluminium part via PEO, then impregnating the coating's open pores with $SrAl_2O_4$: Eu, Dy phosphor powder, and finally sealing the surface with a thin epoxy resin overcoat to secure the ML powder in place. Under mechanical loading, the embedded phosphor emits light in proportion to the local strain, allowing for real time optical stress measurement that can be later extended to 3D stress mapping as shown in [6].

2. MATERIALS AND METHODS

The substrate employed in this study was aluminium alloy Al6082, characterised by a high aluminium content ranging between 95 % and 98 %. The remaining composition included alloying elements such as chromium, copper, iron, magnesium, manganese, and zinc, along with trace quantities of other metals, each present in concentrations varying from 0.1% to 1.3%. These elements contribute to the mechanical strength and corrosion resistance of the alloy, making it suitable for surface modification through plasma electrolytic oxidation (PEO).

For experimental purposes, aluminium sheets with a thickness of 2 mm were sectioned into rectangular samples measuring 55 × 7 × 2 mm³. Each sample had a surface area of 7.97 cm². Prior to undergoing the PEO process, the samples were thoroughly cleaned by rinsing them with ethanol to remove surface contaminants and ensure uniform treatment. After rinsing, the samples were dried under ambient conditions.

PEO surface treatment was performed using a custom-built bipolar electric pulse generator, designated ELGOO PEO V3, rated at 5 kW. This equipment enabled precise regulation of the pulse parameters-including voltage, current, timing, and duty cycle-via an external control interface connected to a personal computer. The operational parameters for sample processing were chosen based on insights from prior investigations, with the specific objective of generating a rough and highly porous surface topology favourable for powder particle entrapment [8].

The electrolyte used for the PEO treatment consisted of a two-component alkaline solution. It was prepared by dissolving potassium hydroxide (KOH) at a concentration of 1 g/L into 650 mL of deionized water. This mixture was subsequently poured into a double-walled water-cooled reactor to maintain thermal stability during processing. To ensure homogeneous mixing, the solution was continuously stirred using a magnetic mixer, and the temperature was regulated and maintained at 20 ± 5 °C throughout the procedure.

During the PEO process, a constant direct current (DC) voltage of 800 V and a stable current of 3 A were applied. No bias voltage was introduced, aligning with prior research that found a pure DC regime encourages the development of a highly porous surface structure. Samples were processed for 15 minutes. For this study, monoclinic $SrAl_2O_4$ powder activated with 1 at% Eu^{2+} and 2 at% Dy^{3+} (sourced from Sigma-Aldrich) was selected as the functional additive.

Following the PEO treatment, the substrates were air-dried under ambient conditions. The $SrAl_2O_4$: Eu, Dy powder was gently rubbed across the surface, ensuring coverage, and any excess was removed by rinsing. Initial tests were conducted on the untreated coated surfaces. Subsequently, a thin layer of epoxy resin was applied to seal the surface and assess the effect of the glaze on performance (Fig. 1).

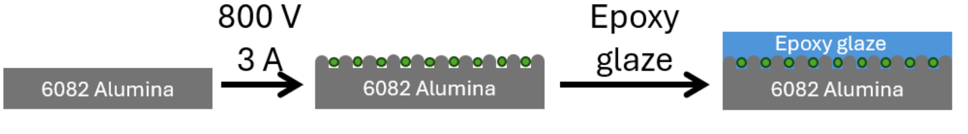

Fig. 1. Graphical representation of sample preparation steps.

Mechanoluminescence measurements were conducted using a custom-built apparatus configured for three-point flexural testing. Detailed schematics and operational principles of the setup are available in our previous study [9]. The device features a stepper motor coupled with a planetary gearset, delivering precise incremental deflection of 6 ± 2 μm per step. Samples were subjected to five displacement levels: 100, 200, 300, 400, and 500 steps-corresponding to nominal deflections of 0.63, 1.27, 1.90, 2.54, and 3.17 mm, respectively.

Samples were excited by a wide spectrum UVA LED. Luminescence was primarily recorded using a photomultiplier tube (PMT) to capture emission intensity before, during and after deflection. Complementary analysis of strain distribution plausibility was performed using a 16-bit CMOS camera (Blackfly BFLY-U3-23S6N). The system was operated at 2 frames per second to improve the signal-to-noise ratio and increase spatial accuracy.

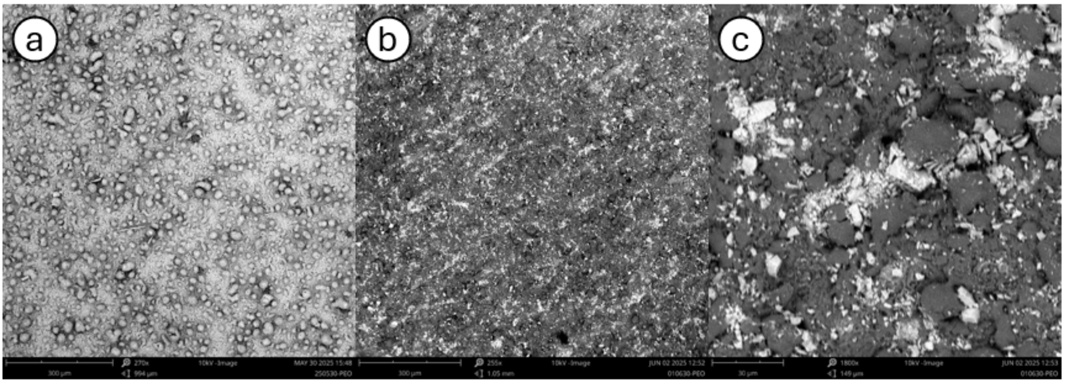

Fig. 2. SEM images of the substrate surface captured at varying stages and magnifications:
a) Post-PEO process at 270× magnification,
b) After application of $SrAl_2O_4$: Eu, Dy powder at 255× magnification,
c) High-resolution view at 1800× magnification.

3. RESULTS

The initial phase of the study aimed to achieve mechanoluminescence from $SrAl_2O_4$: Eu, Dy particles embedded within the PEO layer, without applying an epoxy overlay. Figure 3 presents a comparison of the most responsive sample: a) without epoxy, and b) with epoxy coating. During mechanoluminescence measurements, samples were subjected to mechanical strain beginning at 20 seconds and unloaded at 40 seconds from the start of acquisition. The luminescence intensity exhibited two quasi-linear increases: the first occurred during the loading phase, and the second appeared during unloading. Notably, the peak associated with the unloading phase became prominent only at deflection levels exceeding 1.90 mm, suggesting a strain-dependent activation threshold.

Samples lacking the epoxy glaze did not exhibit mechanoluminescent activity during outward deflection. A negligible increase in luminescence was observed only at deflection levels exceeding 2.54 mm. This lack of response may stem from the microstructure expanding outward during loading, which potentially prevents any mechanical force from being exerted directly onto the phosphor particles.

It is hypothesized that under compressive or shear deformation, the porous microstructure may collapse inward, thereby exerting sufficient force on the particles to activate luminescence. Such behaviour could mimic or even surpass the effect seen in epoxy-coated samples. In the epoxy-glazed case, particle activation likely arises from compressive stress between the embedded phosphors and the rigid epoxy matrix-effectively translating mechanical strain into luminescent output.

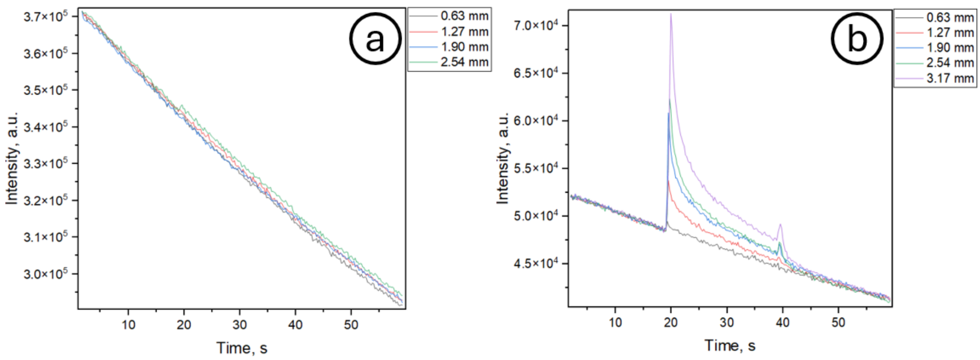

Fig. 3. Typical luminescence intensity during three-point flexural testing for: a) $SrAl_2O_4:Eu^{2+}$, Dy^{3+} phosphors embedded in the PEO structure, and b) particles in a PEO structure with a thin epoxy glaze.

To quantitatively assess the mechanoluminescence response during flexural deformation, an arbitrary contrast ratio was introduced. In this study, the contrast ratio is defined as the difference between the peak luminescence intensity observed during deflection and the minimum baseline intensity recorded prior to force application. This difference is then normalized by the baseline value and expressed as a percentage, representing the relative increase in signal attributable to mechanical stimulation. The minimum baseline intensity corresponds to the residual afterglow of $SrAl_2O_4:Eu^{2+}$, Dy^{3+} particles and is treated as background luminescence.

An example illustrating the contrast ratio calculation is presented in Fig. 4a. Contrast ratios corresponding to each tested deflection step are summarised in Fig. 4b. Although the experiment was designed to operate within the elastic deformation regime of alumina, samples exhibited signs of mechanical fatigue following deflections larger than 3 mm. The diminished signal may be attributed to physical changes in the composite structure-specifically, potential delamination of the epoxy glaze or microstructural degradation within the PEO layer. Despite these findings, no visible or permanent deformation was detected upon visual inspection.

To enable detectable mechanoluminescence, $SrAl_2O_4:Eu^{2+}$, Dy^{3+} particles must first be photoexcited. Therefore, a key parameter investigated was the relationship between the previously defined contrast ratio and the delay interval, i.e., the time between optical excitation and mechanical deformation. In this study, samples were irradiated using a UVA diode for 3 minutes to achieve photoluminescence saturation. Following irradiation, a controlled pause or delay was introduced prior to initiating the mechanoluminescence measurement.

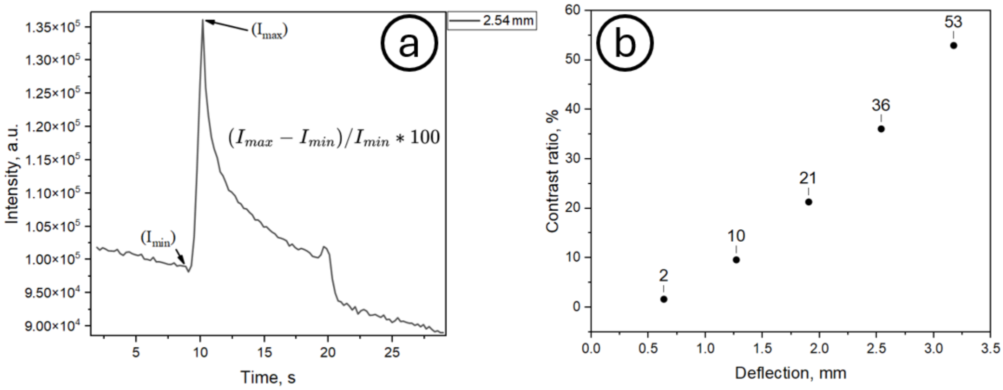

Fig. 4. a) Illustration of the contrast ratio calculation method;
b) graphical representation of the contrast ratios obtained for tested deflection levels.

Background luminescence was recorded for 10 seconds, after which samples were mechanically strained at the 10-second mark and unloaded at 20 seconds. A deflection of 1.97 mm was selected to avoid structural degradation associated with larger displacements. Delay intervals ranging from 10 seconds to 21 minutes were investigated to evaluate the correlation with mechanoluminescence contrast ratio. A visualisation of these findings is provided in Fig. 5a.

For comparative purposes, mechanoluminescence in Fig. 5b is defined as the absolute intensity difference between I_{max} (peak during deformation) and I_{min} (baseline prior to force application). The overall emission intensity decreased exponentially with increasing delay time, consistent with the known afterglow decay behaviour of $SrAl_2O_4$:Eu^{2+}, Dy^{3+}. Mechanoluminescent emission similarly declined with time; however, the calculated contrast ratio remained relatively stable, averaging around 20 %. It is worth noting that data variability may stem from a combination of factors, including intrinsic fluctuations in particle response and changes in external conditions, such as ambient temperature and lighting, during the prolonged acquisition process.

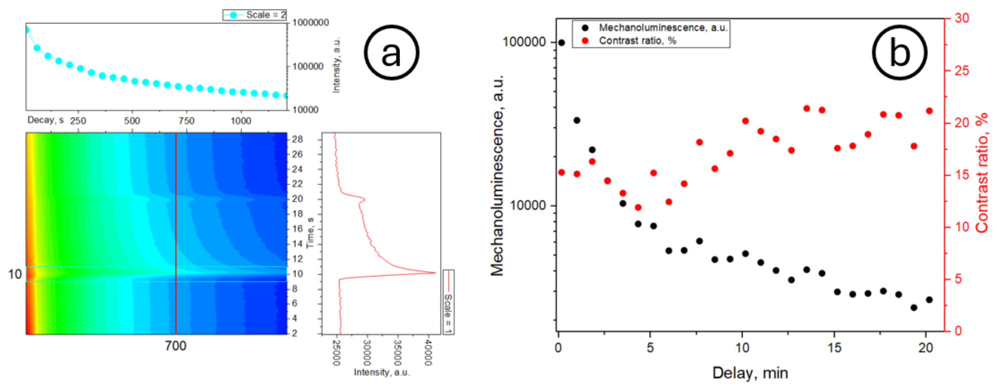

Fig. 5. a) Graphical representation of the acquired luminescence intensity data plotted on an exponential scale, illustrating decay behaviour of $SrAl_2O_4$:Eu^{2+}, Dy^{3+} after UVA excitation over varying delay intervals;
b) Relationship between delay time and mechanoluminescence intensity ($I_{max} - I_{min}$), alongside the corresponding contrast ratio.

To evaluate the practical viability of $SrAl_2O_4:Eu^{2+}$, Dy^{3+} particles embedded in the PEO layer for mapping strain distribution, a CMOS camera was employed. Samples were irradiated for 75 seconds, followed immediately by the mechanoluminescence measurement without delay. Samples were deflected by 3.17 mm.

Figure 6 displays both the integrated luminescence distribution recorded across the substrate surface and the corresponding calculated stress-strain map. The computational method for stress analysis is detailed in our previous study [6].

Mechanoluminescent signals were readily captured by the CMOS camera, with repeated trials revealing a distinct rise in localized luminescence at the centre of the sample, coinciding with the position of the loading pin. However, the overall intensity distribution appeared noisy and difficult to interpret. This variability may result from inhomogeneous particle dispersion, inconsistencies in surface geometry, or uneven exposure to excitation.

While the technique shows promise when compared to theoretical strain distribution [10] for surface-wide strain mapping, further optimisation is necessary to refine surface morphology and improve light yield under deformation.

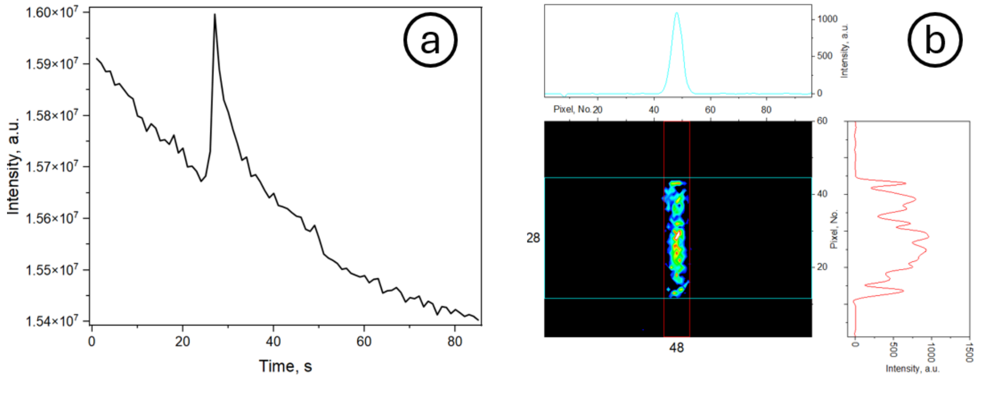

Fig. 6. a) Integrated luminescence captured using a 16-bit CMOS camera during three-point flexural deformation; b) calculated stress-strain distribution map illustrating regions of potential particle activation under compressive and tensile strain.

To evaluate the influence of PEO processing duration on surface morphology and particle retention, several time intervals were examined. Processing times shorter than 15 minutes resulted in brittle coatings with poor particle adherence, leading to inadequate mechanoluminescence performance.

Figure 7 illustrates the typical surface morphology of samples processed for 30 minutes. These samples exhibited a heterogeneous structure, featuring a mix of highly porous regions and dense, low-porosity zones. In contrast, samples treated for 45 minutes developed a consistently low-porosity surface, which failed to retain a sufficient quantity of luminescent particles and were therefore excluded from a mechanoluminescence analysis.

Among the tested durations, a 15-minute processing time proved optimal for substrates with an approximate surface area of 8 cm^2, balancing porosity, structural integrity, and particle retention for effective mechanoluminescence functionality.

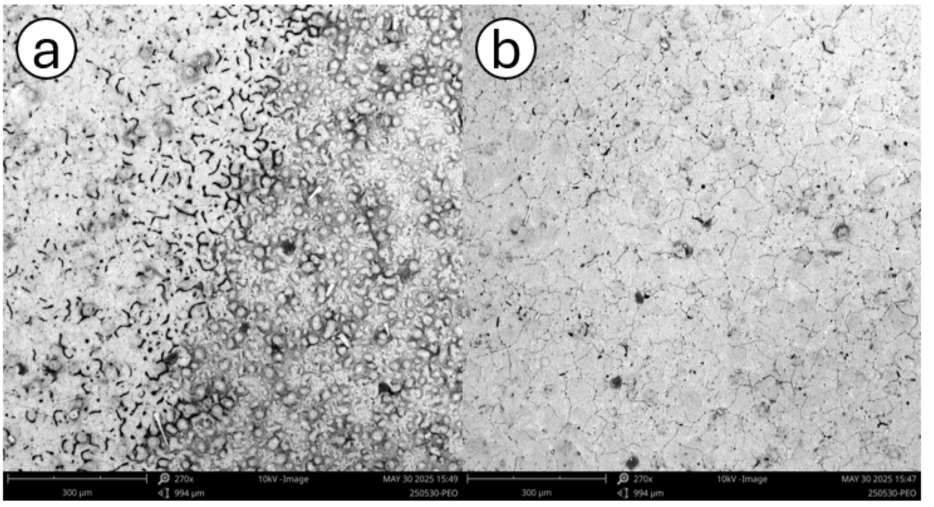

Fig. 7. a) Surface morphology of samples processed via PEO for 30 minutes and b) 45 minutes.

4. DISCUSSION

The results of this study demonstrate that mechanoluminescent sensing can be successfully integrated into PEO modified aluminium surfaces, but the performance strongly depends on the microstructural characteristics of the oxide layer and the mechanical coupling between the phosphor particles and the surrounding matrix. The porous alumina produced by a 15minute PEO treatment provided the most favourable balance between porosity and structural integrity, enabling sufficient particle retention while maintaining mechanical robustness during flexural loading. Longer PEO durations resulted in either heterogeneous or overly dense surfaces, both of which hindered particle incorporation and reduced mechanoluminescent output.

A key finding is the distinct difference in mechanoluminescent behaviour between uncoated and epoxy sealed samples. Without epoxy, the PEO microstructure appears to deform outward during bending, reducing the effective force transmitted to the embedded phosphors. Only at higher deflections – where local collapse or shear of the porous network likely occurs – a luminescent response is measurable. This suggests that the mechanical activation of particles in a purely porous ceramic matrix is highly sensitive to local deformation and may require specific pore geometries or particle-pore interactions to achieve consistent activation.

In contrast, the epoxy sealed samples exhibited clear and repeatable mechanoluminescent signals during both loading and unloading. The epoxy layer likely acts as a rigid mechanical intermediary, transferring compressive stress directly onto the phosphor particles. This behaviour aligns with previous observations in polymer-phosphor composites, where mechanoluminescence is driven by particle-matrix compression. The presence of two linear luminescence peaks – one during loading and one during unloading – further supports the idea that particle activation is governed by relative motion or stress gradients rather than absolute strain alone.

The stability of the contrast ratio across a wide range of delay intervals is particularly promising for practical sensing applications. Although the absolute luminescence intensity decays exponentially due to the afterglow characteristics of $SrAl_2O_4:Eu^{2+}$, Dy^{3+}, the relative mechanoluminescent response remains nearly constant. This indicates that the ML signal is not strongly dependent on the absolute trap population, but rather on the incremental release of charge carriers triggered by mechanical stimulation. Such behaviour suggests that MLbased stress sensing could remain effective even when excitation conditions vary or when long-term monitoring is required.

However, several limitations were identified. Mechanical fatigue at higher deflections reduced signal reproducibility, likely due to microcracking, partial delamination of the epoxy glaze, or degradation of the PEO layer. Additionally, CMOS imaging revealed that spatial mapping of strain is feasible but currently limited by particle inhomogeneity and surface roughness, which introduce noise into the luminescence distribution. These findings highlight the need for improved particle infiltration strategies, controlled pore architectures, and optimized sealing layers to achieve uniform and highcontrast stress maps.

Therefore, the study confirms the feasibility of embedding mechanoluminescent particles into PEO coatings for optical stress sensing, while also identifying key microstructural and mechanical factors that must be addressed to advance the technique toward practical implementation.

5. CONCLUSIONS

This study has demonstrated a proofof-concept method for integrating mechanoluminescent stress sensing into aluminium components using plasma electrolytic oxidation. The study shows that PEO coatings can successfully incorporate $SrAl_2O_4:Eu^{2+}$, Dy^{3+} particles, although the resulting morphology depends strongly on processing time; a 15 minute treatment yields the most favourable porosity for both particle retention and mechanical stability. When the particles are embedded directly within the PEO layer, their mechanoluminescent output remains limited, likely because bending causes outward expansion of the porous structure. As a result, measurable signals emerge only at higher deflections where localized pore collapse or shear takes place. Introducing a thin epoxy glaze dramatically improves performance, producing clear and repeatable luminescent peaks during both loading and unloading by enhancing mechanical coupling between the substrate and the phosphor particles.

The contrast ratio of the mechanoluminescent response remains stable even after long delays, indicating that the relative signal is resilient to afterglow decay and suitable for time-dependent sensing applications. CMOS imaging further demonstrates the feasibility of spatial strain mapping, though better particle distribution and surface uniformity are needed to reduce noise and improve interpretability. The experiments also reveal that mechanical fatigue at large deflections diminishes signal reliability, highlighting the need for future improvements in coating toughness and adhesion. Overall, embedding mechanoluminescent particles into PEO modified aluminium surfaces offers a promising route toward wirefree, fullfield stress visualization in metal components, and continued refinement of coating morphology, particle infiltration, and surface sealing will be crucial for advancing this technique in structural health monitoring and other engineering applications.

ACKNOWLEDGEMENT

The research has been conducted based on an agreement with Ltd. ETKC (Centre of Competence for Energy and Transportation) within the framework of the project No. 5.1.1.2.i.0/2/24/A/CFLA/002 - co-funded by the Recovery and Resilience Facility.

Institute of Solid State Physics, University of Latvia as the centre of Excellence has received funding from the European Union's Horizon 2020 Framework Programme H2020-WIDESPREAD-01-2016-2017-TeamingPhase2 under grant agreement No. 739508, project CAMART2.

REFERENCES

1. James, M.N., Hughes, D.J., Chen, Z., Lombard, H., Hattingh, D. G., Asquith, D., … & Webster, P.J. (2007). Residual stresses and fatigue performance. *Eng Fail Anal, 14*(2), 384–395. https://doi.org/10.1016/J.ENGFAILANAL.2006.02.011
2. Chiocca, A., Frendo, F., & Bertini, L. (2022). Residual stresses influence on the fatigue strength of structural components. *Procedia Structural Integrity, 38*, 447–456. https://doi.org/10.1016/J.PROSTR.2022.03.045
3. Zhuang, Y., & Xie, R. J. (2021). Mechanoluminescence rebrightening the prospects of stress sensing: A review. *Advanced Materials, 33*(50), 2005925. https://doi.org/10.1002/ADMA.202005925
4. Timilsina, S., Sohn, K.-S., Park, W. B., & Kim, J. S. (2014). Mechanoluminescence of SrAl2O4:Eu2+, Dy3+ under cyclic loading. *Optics Letters, 39*(6), 1410–1413. https://doi.org/10.1364/OL.39.001410
5. Einbergs, E., Spustaka, A., Vitola, V., & Zolotarjovs, A. (2023). By visualizing the deformation with mechanoluminescent particles, additive manufacturing offers a practical alternative to stress and strain simulation. *Designs, 7*(2), Article 54. https://doi.org/10.3390/DESIGNS7020054
6. Einbergs, E., Zolotarjovs, A., Bite, I., Vītola, V., Spustaka, A., Tunēns, G., & Arnautov, A. (2022). A mechanoluminescence-based approach to spatial mechanical stress visualisation of additively manufactured (3D printed) parts. *Materialia, 24*, Article 101516. https://doi.org/10.1016/J.MTLA.2022.101516
7. Adelinia, A., Yerokhin, A., Matthews, D. T. A., de Rooij, M. B., & Seyyed Monfared Zanjani, J. (2025). Pore formation and pore inter-connectivity in plasma electrolytic oxidation coatings on aluminium alloy. *Surf Coat Technol, 496*, Article 131597. https://doi.org/10.1016/J.SURFCOAT.2024.131597
8. Auzins, K., Zolotarjovs, A., Bite, I., Laganovska, K., Vitola, V., Smits, K., & Millers, D. (2019). Production of phosphorescent coatings on 6082 aluminum using Sr0.95Eu0.02Dy0.03Al2O4-δ powder and plasma electrolytic oxidation. *Coatings, 9*(12), Article 865. https://doi.org/10.3390/COATINGS9120865
9. Einbergs, E., & Zolotarjovs, A. (2022). Programmable material testing device for mechanoluminescence measurements. *HardwareX, 12*, Article e00349. https://doi.org/10.1016/J.OHX.2022.E00349
10. Efe, T., Sengun, N., Demirdag, S., Tufekci, K., & Altindag, R. (2019). Effect of sample dimension on three and four points bending tests of fine crystalline marble and its relationship with direct tensile strength. *IOP Conf Ser Earth Environ Sci, 221*(1), 012093. https://doi.org/10.1088/1755-1315/221/1/012093